Dalton Transactions

Accepted Manuscript

ROYAL SOCIETY OF CHEMISTRY

www.rsc.org/dalton

Journal Name

RSCPublishing

ARTICLE

Cite this: DOI: 10.1039/x0xx00000x

Received 00th January 2012,
Accepted 00th January 2012

DOI: 10.1039/x0xx00000x

www.rsc.org/

Fabrication and optical nonlinearities of composite films derived from the water-soluble Keplerate-type polyoxometalate and the chloroform-soluble porphyrin

Zonghai Shi,[a] Yunshan Zhou,[*a,b] Lijuan Zhang,[*a] Di Yang,[a] Cuncun Mu,[a] Haizhou Ren[a], Farooq Khurum Shehzad[a] and Jiaqi Li[a]

Composite films derived from the water-soluble Keplerate-type polyoxometalate $(NH_4)_{42}[Mo_{132}O_{372}(CH_3COO)_{30}(H_2O)_{72}]$·*ca*·$300H_2O$·*ca*·$10CH_3COONH_4$ (denoted $(NH_4)_{42}\{Mo_{132}\}$) and chloroform-soluble tetraphenylporphyrin perchlorate $[H_2TPP](ClO_4)_2$ are successfully fabricated by layer-by-layer self-assembly method and characterized by UV–vis. spectroscopy and X-ray photoelectron spectroscopy (XPS). The structure of the $\{Mo_{132}\}$ and $[H_2TPP]^{2+}$ in the films keep intact in light of the results of UV–vis. spectroscopy and XPS. UV-vis. spectra measurements reveal that the amounts of deposition of $\{Mo_{132}\}$ and $[H_2TPP]^{2+}$ remain constant in every adsorption cycle in the composite films assembly process. Nonlinear optical properties of the composite films have been investigated by using the Z-scan technique at a wavelength of 532 nm and pulse width of 7 ns. The results show that the composite films have notable nonlinear saturated absorption and self-defocusing effects. The combination of $\{Mo_{132}\}$ with $[H_2TPP]^{2+}$ can result in the composite films with remarkably enhanced optical nonlinearities. The interfacial charge transfer induced by laser from porphyrin to POM in the films is thought to play key role in the enhancement of NLO response. The third-order NLO susceptibility $\chi^{(3)}$ of the composite films increases with the increase of film thickness.

1. Introduction

Development of materials with promising nonlinear optical (NLO) responses has attracted considerable attention because of their potential applications in the domain of photoelectronics and photonics.[1-3] In the last two decades there has been much interest in the NLO properties of organic materials, particularly with the structure of extensively delocalized π-electrons, due to their large NLO susceptibilities, architectural flexibility and their potential application as NLO material.[4,5] Among different organic materials, porphyrin and their derivatives generally exhibiting remarkable reverse saturable absorption (RSA) properties have been proved to be a class of most promising third-order NLO materials and have attracted significant research interests in the field of nonlinear optics in recent years due to their fast NLO response speed and unique architectural flexibility.[1,7-12]

On the other hand, polyoxometalates (POMs), a class of metal–oxygen cluster compounds having remarkable structural diversity and variety in chemical composition, are attractive building blocks for functional supramolecular materials with potential applications in electrocatalytic, molecular electronic and electrooptical devices.[13] Among all types of POMs, the Keplerate-type POM with a general formula $[Mo_{132}O_{372}(L)_{30}(H_2O)_{72}]^{n-}$ (L = CH_3COO^-, SO_4^{2-}, $HCOO^-$, et al) belongs to a family of molecular metal-oxide-based clusters with spherical periodicity.[14] It features a capsule with the size of 2.9 nm, 20 $\{Mo_9O_9\}$ pores and a cavity connected to the outside via 20 channels, its inner shell can be modified by various ligands like CH_3COO^-, HPO_2^-, PO_4^{3-} and SO_4^{2-}, corresponding to different anionic charges and as a consequence different affinity to/and a different number of cations. Besides, it comprises 72 Mo^{VI} atoms with empty 4d orbit and 60 Mo^{V} atoms, and belongs to the type I category within the Robin-Day classification for mixed-valence compounds. This character is thought to be very important in view of NLO science because it may result in extensive polarization of charge and consequently would bring good NLO response when the molecules are exposed to electromagnetic

radiation, as confirmed by our previous experimental results.[15-18]

Considering the fact that both porphyrin and Keplerate-type of POMs are versatile in NLO fields, modulation and/or enhancement of NLO responses is greatly expected by integrating the Keplerate-type of POMs and porphyrin leading to the porphyrin-POM hybrid. However, the adverse solubility (hydrophilic *vs* hydrophobic) of these two moieties makes the synthesis of such hybrid materials extremely difficult using traditional solution methods, which definitely hinders the development of porphyrin-POM-based NLO materials.[19] Fortunately, a simple yet versatile layer-by-layer self-assemble method offers a chance to meet this challenge. It offers the ability to exert molecular-level control over architecture, composition, and thickness of the assembled thin films and has been widely used in the field of optoelectronic devices.[20] In particular, it has the ability to fabricate multilayer thin films in different solvents (organic or aqueous) and provides a solution to the problem of incorporating compounds which cannot be dissolved in same solvent into a LBL self-assembled film.[21]

Based on the above analysis and following our continuous efforts towards investigating NLO properties of porphyrin-POM-based materials and their consequent practical applications,[15-18,22,23] in this paper, we report the fabrication, characterization and third-order NLO properties of the LBL composite films derived from the water-soluble Keplerate-type polyoxometalate $(NH_4)_{42}[Mo_{132}O_{372}(CH_3COO)_{30}(H_2O)_{72}]\cdot ca\cdot 300H_2O\cdot ca\cdot 10CH_3COONH_4$ (denoted $(NH_4)_{42}\{Mo_{132}\}$, Fig. 1A) and chloroform-soluble tetraphenylporphyrin perchlorate $[H_2TPP](ClO_4)_2$ (Fig. 1B).

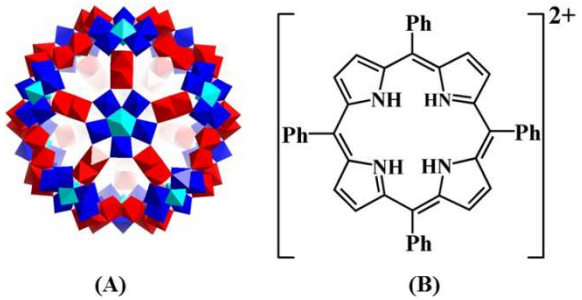

Fig. 1 Structures of the Keplerate-type polyoxometalate anion $\{Mo_{132}\}$ (A) and divalent cations of porphyrin $[H_2TPP]^{2+}$ (B) used in this study

2. Experimental

2.1 Instruments and Material

IR spectra were recorded on a MAGNA-IR 750 (Nicolet) spectrophotometer with KBr pellet in the 400 – 4000 cm^{-1} region. The UV-vis. spectra were recorded with a Shimadzu UV-2550 spectrophotometer in the range of 200 – 800 nm. XPS spectra were recorded with ESCALABMK-2 electron spectrometer (VG Scientific Ltd., UK). Cyclic voltammograms (CV) were obtained on a CHI660B electrochemical analyzer at room temperature at the rate of 10 mV/s. NLO properties were performed by using an EKSPLA NL303 Q-switched Nd:YAG laser at 532 nm with a pulse duration of τ = 7 ns, a repetition rate of 10 Hz and the intensity of the light at focus E_0 being 20 μJ. The waist ω_0 was measured to be 19 μm. The linear transmittance of the far-field aperture S was measured to be 0.25. The samples were proved to be stable towards air and laser light under the experimental conditions. Before the measurements, the system was calibrated using CS_2 as reference.

$(NH_4)_{42}\{Mo_{132}\}$ and $[H_2TPP](ClO_4)_2$ were prepared according to the literature method,[14,23] and characterized by IR and UV-vis. spectra (Electronic Supplementary Information, Fig. S1 – Fig. S4). Poly(allylamine hydrochloride) (PAH; MW 15000 g/mol), poly(styrene sulfonate) (PSS; MW 70000 g/mol) and all the other chemicals and reagents were purchased from Aladdin, were of analytical grade and used without further purification. Ultra-pure water was used for all aqueous solutions preparation.

2.2 Fabrication of ultrathin multilayer films

Quartz wafers were cleaned in a piranha solution (H_2SO_4/H_2O_2, 70/30, V/V) at 80 °C for 1 h, then rinsed with copious water and dried under a nitrogen stream. This procedure results in a hydrophilic substrate surface. The cleaned substrates were immersed in an aqueous solution of PAH (10^{-3} mol/L) for 10 min., rinsed with copious water and dried under nitrogen stream. The PAH coated substrates were exposed to a PSS solution (10^{-3} mol/mL, pH ≈ 3 adjusted by using 0.5 mol/L HCl) for 10 min., rinsed with copious water and dried under nitrogen stream. After that, the substrate was soaked in the $[H_2TPP](ClO_4)_2$ solution (in $CHCl_3$, 10^{-3} mol/L) for 10 min, followed by rinsing with $CHCl_3$ to remove the excess nonbounded porphyrin. Subsequently, a layer of POM was attached by soaking the substrate for 10 min. in a $(NH_4)_{42}\{Mo_{132}\}$ aqueous solution (10^{-3} mol/L, pH ≈ 4 adjusted by using 0.5 mol/L HCl) and rinsed with water. After each rinsing, the films were dried by nitrogen. The procedure was repeated until the desired film thickness was obtained, thus resulting in formation of the composite films $(PAH/PSS)(H_2TPP/\{Mo_{132}\})_n$ (denoted $(H_2TPP/\{Mo_{132}\})_n$).

The films $(PAH/PSS)(PAH/\{Mo_{132}\})_n$ (denoted $(PAH/\{Mo_{132}\})_n$) and $(PAH/PSS)(H_2TP/PSS)_n$ (denoted $(H_2TP/PSS)_n$) were built up by alternating 10 min immersion of the precursor film coated substrate in PAH + $(NH_4)_{42}\{Mo_{132}\}$ solution, and $[H_2TPP][ClO_4]_2$ + PSS solution, respectively. Water or $CHCl_3$ rinsing and nitrogen drying steps were performed after each absorption step.

3. Results and discussion

The film's growth process can be monitored by UV-vis. spectroscopy. Fig. 2 shows the UV-vis. spectra of composite films $(H_2TPP/\{Mo_{132}\})_n$ (n = 1 ~ 8) assembled quartz substrates. The spectra exhibit the characteristic absorption bands at 235 nm and 445 nm and 421 nm for $\{Mo_{132}\}$ and $[H_2TPP]^{2+}$ respectively, which confirms the incorporation of $\{Mo_{132}\}$ and $[H_2TPP]^{2+}$ into the multilayers films without any

structural alteration.[14,24] The bands at 235 nm and 445 nm are assigned to charge transfer absorption band of Mo←O_d and

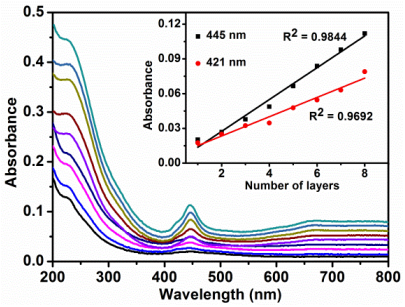

Fig. 2. UV-vis. absorption spectra of $(H_2TPP/\{Mo_{132}\})_n$ (n = 0 ~ 8) depositing on a quartz substrate. The inset shows absorbance at 421 nm and 445 nm versus the layer number of $(H_2TPP/\{Mo_{132}\})_n$ layers.

Mo←$O_{b,c}$ of $\{Mo_{132}\}$ respectively.[25] The shoulder band appear at 421 nm is attributed to Soret band of $[H_2TPP]^{2+}$, the Q bands of porphyrin are too weak to appear in the spectrum. The red shift of the Soret band for $[H_2TPP]^{2+}$ and blue shift of Mo←$O_{b,c}$ for $\{Mo_{132}\}$ comparing with that of parent reactants in solution (Fig. S2 and S4) can be attributed to the strong electronic interaction between the anions $\{Mo_{132}\}$ and the cations $[H_2TPP]^{2+}$ in the densely packed films.[26] The polyanion PSS and polycation PAH shows no absorbance above 200 nm, and their presence in the films does not contribute to the UV-vis. spectra.[27] Importantly, as shown in the inset of Fig. 2, the absorbance at 421 nm and 445 nm versus the layer number of films $(H_2TPP/\{Mo_{132}\})_n$ result in two nearly straight lines, which confirm that the $\{Mo_{132}\}$ anions and $[H_2TPP]^{2+}$ cations are smoothly incorporated into the multilayers and the amounts of deposition of $\{Mo_{132}\}$ and $[H_2TPP]^{2+}$ remain constant in every adsorption cycle in the composite films assembly process as well.

The X-ray photoelectron spectroscopy (XPS) of the film $(H_2TPP/\{Mo_{132}\})_6$ is used to confirm the composition of the composite films. Fig. 3 clearly shows the characteristic Mo_{3d} doublet composed of the $3d_{5/2}$ and $3d_{3/2}$ levels resulting from spin–orbit coupling. Good fitting of the data points is achieved by using two pairs of Lorentzian–Gaussian functions, corresponding to two possible 3d doublets of Mo in different oxidation states, that is, Mo^{VI} and Mo^{V}. The contribution from the Lorentzian–Gaussian peaks centered at 232.6 eV and 235.6 eV are assigned as Mo^{V}, while the peaks at 233.7 eV and 236.8 eV are attributed to Mo^{VI}. The Mo^{V} and Mo^{VI} binding energies match well with the literature values.[28] From semi-quantitative calculation[29] it is known that the characteristic peak area ratio of Mo^{VI} and Mo^{V} is *ca.* 1.2:1, matching very well with 72 Mo^{VI} and 60 Mo^{V} in $\{Mo_{132}\}$ cluster, which further confirms intactness of the structure of $\{Mo_{132}\}$ in $(H_2TPP/\{Mo_{132}\})_n$ films. In addition, the N_{1s} peak with bond energy of 398.8 eV and 401.6 eV is attributed to the protonated nitrogen atom from $[H_2TPP]^{2+}$ and PAH, respectively.[30,31] This indicates that the skeleton of $[H_2TPP]^{2+}$ have been keep intact in $(H_2TPP/\{Mo_{132}\})_n$ films. The XPS data further unequivocally suggests that $\{Mo_{132}\}$ and $[H_2TPP]^{2+}$ have indeed been incorporated successfully into the multilayer films, which is quite in agreement with the result obtained from UV-vis. spectra measurements.

The Z-scan curves along with corresponding fits for composite films $(H_2TPP/\{Mo_{132}\})_n$ (n = 6, 12, 16, 24) are shown in Fig. 4. All of the films have notable nonlinear saturable absorption (SA) under the open-aperture configuration corresponding to a negative nonlinear absorption coefficient β (Fig. 4A). Each of the closed-aperture Z-scan curves for the films have a peak-valley configuration corresponding to a negative nonlinear refractive index and a characteristic self-defocusing behavior of the propagating wave in the films (Fig. 4B).

In order to investigate the contribution of $\{Mo_{132}\}$ and $[H_2TPP]^{2+}$ in the films to the third-order NLO response of the composite films, multilayer films $(PAH/\{Mo_{132}\})_n$ and $(H_2TPP/PSS)_n$ were fabricated and characterized (Electronic Supplementary Information, Fig. S5). Based on the UV-vis. spectra measurement (Fig. 5) where absorbance and concentration of a substance has a direct relationship according to Lambert-Beer law, it was found that the absorption at 445 nm for $(PAH/\{Mo_{132}\})_4$ and 421 nm for $(H_2TPP/PSS)_4$ is almost same with those absorptions in $(H_2TPP/\{Mo_{132}\})_6$ indicating that the amount of $\{Mo_{132}\}$ in $(PAH/\{Mo_{132}\})_4$ and of $[H_2TPP]^{2+}$ in $(H_2TPP/PSS)_4$ is almost the same with those in $(H_2TPP/\{Mo_{132}\})_6$, respectively, which can be explained in view of the much higher negative charges (or charge densities) of PAH and PSS as compared with those of H_2TPP and $\{Mo_{132}\}$.

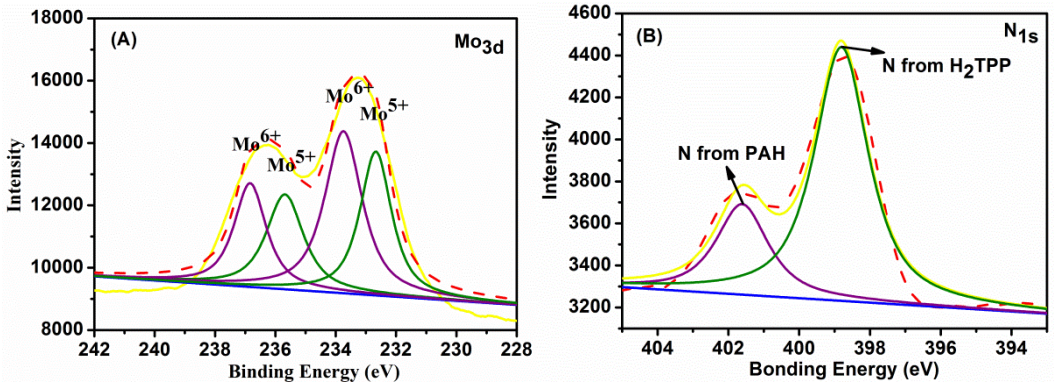

Fig. 3. Mo_{3d} (A) and N_{1s} (B) peaks in the XPS spectra of $(H_2TPP/\{Mo_{132}\})_6$. (The dash lines indicate experimental data and the solid lines indicate fitted curves).

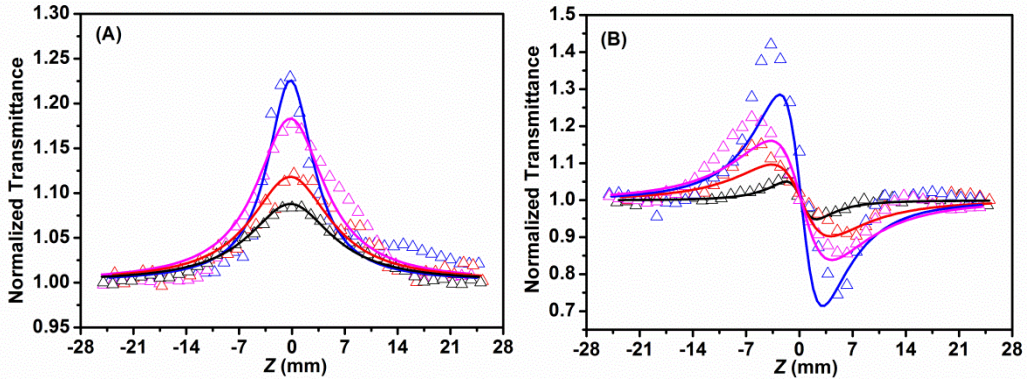

Fig. 4. Z-scan curves of $(H_2TPP/\{Mo_{132}\})_n$ ((A): open-aperture curves; (B): closed-aperture curves; black: n = 6; red: n = 12; pink: n = 16; blue: n = 24, the open triangles indicate the measured data; the solid curves are theoretical fits).

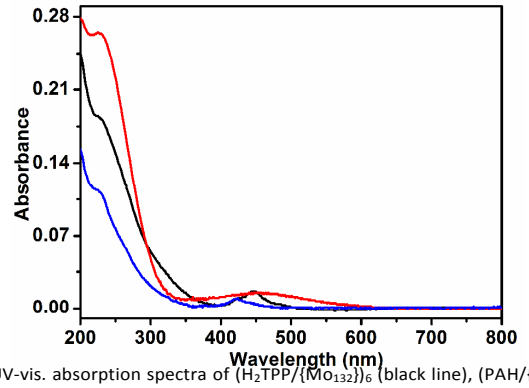

Fig. 5. UV-vis. absorption spectra of $(H_2TPP/\{Mo_{132}\})_6$ (black line), $(PAH/\{Mo_{132}\})_4$ (red line) and $(H_2TPP/PSS)_4$ (blue line).

As we know that the optical nonlinear susceptibility $\chi^{(3)}$ is dependent on the amount of material. Since that the amount of $\{Mo_{132}\}$ in $(PAH/\{Mo_{132}\})_4$ and $[H_2TPP]^{2+}$ in $(H_2TPP/PSS)_4$ is almost the same with those in $(H_2TPP/\{Mo_{132}\})_6$, the amount of $\{Mo_{132}\}$ and $[H_2TPP]^{2+}$ in $(PAH/\{Mo_{132}\})_4$, $(H_2TPP/PSS)_4$ and $(H_2TPP/\{Mo_{132}\})_6$ is thought to have almost same effect on the NLO properties measured under the same experimental conditions. The open-aperture curves of $(PAH/\{Mo_{132}\})_4$ and $(H_2TPP/PSS)_4$ are shown in Fig. 6A, where a single peak at the focus position appears indicating that both of them have notable SA effect. Notably, this is in contrast to the solution of $\{Mo_{132}\}$ which shows negligible nonlinear absorption effect[16] and $[H_2TPP](ClO_4)_2$ which shows notable RSA.[23] The RSA of porphyrin is originating from the occurrence of intersystem crossing from the lowest excited singlet state to the lowest triplet state and the subsequent increase in the population of the strongly absorbing triplet state with nanosecond dynamics.[1] It should be pointed that this kind of transformation in the nonlinear absorption found in the title composite films is also found in the reference,[12] and should be attributed to the surface effect of ultrathin composite film,[32] i.e., the excited electrons introduced by laser would be trapped by the surface state in the film rather than the excited state. The self-defocusing behavior are found in $(PAH/\{Mo_{132}\})_4$ and $(H_2TPP/PSS)_4$ (Fig. 6B). The PAH, PSS and their compositions do not have NLO effect under the same experimental conditions,[33] therefore, both the observed NLO response in the composite films are just attributed to the contribution of the POMs and porphyrin components.

The following formula are used to calculate the third-order nonlinear refractive index n_2 (esu), nonlinear absorption coefficient β (esu) and optical nonlinear susceptibility $\chi^{(3)}$ (esu).[34]

$$\Delta T_{P-V} = 0.406(1-S)^{0.25}\left|\Delta\phi_0\right| \quad (1)$$

$$\Delta\phi_0 = kL_{\text{eff}}\gamma I_0 \quad (2)$$

$$L_{\text{eff}} = (1-e^{-\alpha_0 L})/\alpha_0 \quad (3)$$

$$n_2(esu) = \frac{cn_0}{40\pi}\gamma(m^2/W) \quad (4)$$

where, ΔT_{P-V} is the normalized peak-valley difference, $\Delta\varphi_0$ is the phase shift of the beam at the focus, $K = 2\pi/\lambda$ is the wave vector, I_0 (unit: W/m^2) is the intensity of the light at focus, L_{eff} is the effective length of the sample defined in terms of the linear-absorption coefficient α_0 and the true optical path length through the sample, n_0 is the linear refractive index, and γ is optical Kerr constant. The conversion can be realized between n_2 (esu) and γ (m^2/W) by eq (4).

Journal Name RSCPublishing

ARTICLE

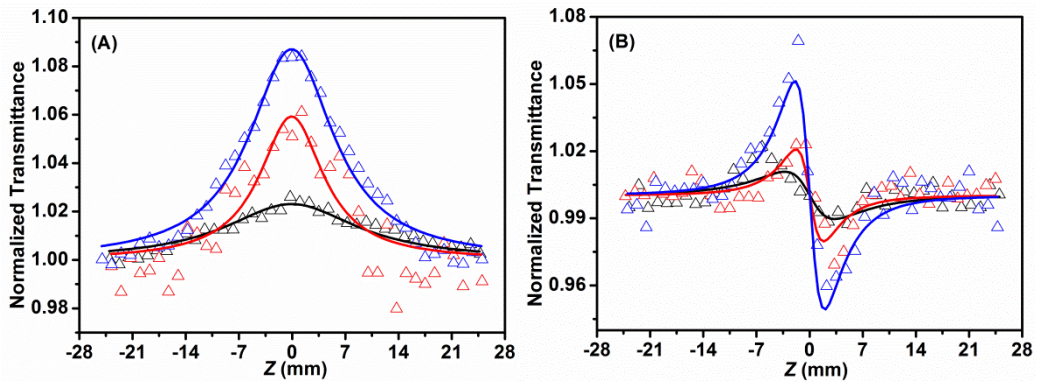

Fig. 6. Z-scan curves of $(H_2TPP/PSS)_4$ (black line), $(PAH/\{Mo_{132}\})_4$ (red line) and $(H_2TPP/\{Mo_{132}\})_6$ (blue line). ((A): open-aperture curves; (B): closed-aperture curves; the open triangles indicate the measured data; the solid curves are theoretical fits)

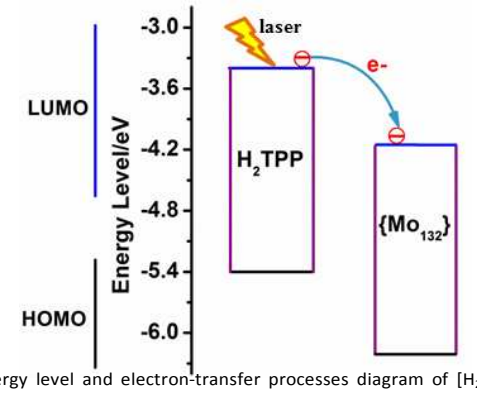

Fig. 7. Energy level and electron-transfer processes diagram of $[H_2TPP](ClO_4)_2$, $\{Mo_{132}\}$ molecules. Color code: blue, LUMO level; black, HOMO level.

When the sample is measured under open aperture, the normalized transmittance T (z, s = 1) can be expressed as

$$T(z, s=1) = \sum_{m=0}^{\infty} \frac{[-q_0(z)]^m}{(m+1)^{3/2}} \quad (5)$$

where $q_0(z) = \frac{\beta I_0 L_{eff}}{(1+z^2/z_0^2)}$, β is nonlinear absorption coefficient. From eq (5) we can get β. From eq (6), we can get the third-order optical nonlinear susceptibility $\chi^{(3)}$.

$$\chi^{(3)} = \sqrt{(\frac{cn_0}{160\pi^2}\gamma)^2 + (\frac{c\beta n_0^3 \lambda}{64\pi^3})^2} \quad (6)$$

Using eqs (4), (5) and (6), the nonlinear refractive index n_2, nonlinear absorption coefficient β and third-order optical nonlinear susceptibility $\chi^{(3)}$ are calculated (Table 1). Data in Table 1 obviously show that $(H_2TPP/\{Mo_{132}\})_6$ demonstrates much better NLO properties compared with those of $(H_2TPP/PSS)_4$ and $(PAH/\{Mo_{132}\})_4$. The optical nonlinear susceptibility $\chi^{(3)}$ of $(H_2TPP/\{Mo_{132}\})_6$ is larger than that of both $(H_2TPP/PSS)_4$ and $(PAH/\{Mo_{132}\})_4$, and even larger than the algebraic sum of those of $(H_2TPP/PSS)_4$ and $(PAH/\{Mo_{132}\})_4$ indicating that combination of POMs with porphyrin can obtain the composite films with improved NLO properties, although the driving force of the combination only depends on the electrostatic interaction between $[H_2TPP]^{2+}$ and $\{Mo_{132}\}$.

Table 1. The experimental Z-scan results for the $(H_2TPP/PSS)_4$, $(PAH/\{Mo_{132}\})_4$ and $(H_2TPP/\{Mo_{132}\})_n$ (n = 6, 12, 16, 24) films.

Samples	$\beta \times 10^{-5}$ (esu)	$n_2 \times 10^{-10}$ (esu)	$\chi^{(3)} \times 10^{-11}$ (esu)
$(H_2TPP/PSS)_4$	-0.052	-0.123	0.198
$(PAH/\{Mo_{132}\})_4$	-0.110	-0.175	0.301
$(H_2TPP/\{Mo_{132}\})_6$	-0.170	-0.312	0.521
$(H_2TPP/\{Mo_{132}\})_{12}$	-0.238	-0.767	1.076
$(H_2TPP/\{Mo_{132}\})_{16}$	-0.360	-1.152	1.551
$(H_2TPP/\{Mo_{132}\})_{24}$	-0.454	-2.118	2.784

The photoinduced interfacial electron transfer from the H_2TPP to $\{Mo_{132}\}$ clusters should be responsible for such enhancement of the NLO properties.[35,36] Since the LUMO level of the $\{Mo_{132}\}$ (Electronic Supplementary Information) is lower than that of the H_2TPP,[23] the excited electrons could inject from the H_2TPP to the $\{Mo_{132}\}$ (Fig. 7). The excited electron transfer can reduce the recombination of electrons and holes in the nano-ultrathin films,[26,35] which will result in larger charge carrier lifetime, leads to the enhanced nonlinear optical

properties.[35,37] Thus, the porphyrin-POM composite films certainly display higher NLO response than that of the $(H_2TPP/PSS)_4$ and $(PAH/\{Mo_{132}\})_4$ films. In addition, data in Table 1 also demonstrates that the third-order NLO susceptibility $\chi^{(3)}$ of $(H_2TPP/\{Mo_{132}\})_n$ (n = 6, 12, 16, 24) increases with the increase of film thickness.

4. Conclusion

In conclusion, novel porphyrin-POMs composite films showing strong self-defocusing features and notable nonlinear saturated absorption are successfully fabricated by layer-by-layer assemble method. The porphyrin-POMs composite films show enhanced NLO properties compared with that of films derived from the porphyrin+PSS and POMs+PAH. The enhancement in the optical nonlinearity should be attributed to the interfacial charge transfer between porphyrin and POMs in the films. Moreover, the third-order NLO susceptibility $\chi^{(3)}$ increases with the increase of film thickness, indicating that materials with expected third-order nonlinear susceptibility can be easily obtained by adjusting the layers of the films in order to meet the virtual needs. Although the $\chi^{(3)}$ value is not large enough for device application, the fact that the combination of POM anions with porphyrin cations, which are not available in same solvent, can obtain the composite films via layer-by-layer method with enhanced optical nonlinearity, informs us of a new convenient approach to explore porphyrin-POM-based NLO materials. The present work also donates important insight into the NLO properties of porphyrin−POM composite films.

Acknowledgements

The financial support of the NSFC and PCSIRT (No. IRT1205) and Beijing Engineering Center for Hierarchical Catalysts is greatly acknowledged. Prof. Xue Duan of Beijing University of Chemical Technology is greatly acknowledged for his kind support.

Notes and references

[a] State Key Laboratory of Chemical Resource Engineering, Institute of Science, Beijing University of Chemical Technology, Beijing 100029, P. R. China.

[b] Laboratory of Optical Physics, Institute of Physics, Chinese Academy of Sciences, Beijing 100190, P. R. China.

Electronic Supplementary Information (ESI) available: detailed IR spectra, UV-vis., CV spectra. See DOI: 10.1039/b000000x/

*Corresponding author. Tel.: +86-10-64414640; e-mail: zhouys@mail.buct.edu.cn; ljzhang@mail.buct.edu.cn

1. M. O. Senge, M. Fazekas, E. G. A. Notaras, W. J. Blau, M. Zawadzka, O. B. Locos and E. M. N. Mhuircheartaigh, *Adv. Mater.*, 2007, **19**, 2737.
2. N. Jiang, G. Zuber, S. Keinan, A. Nayak, W. Yang, M. J. Therien and D. N. Beratan, *J. Phys. Chem. C*, 2012, **116**, 9724.
3. T. V. Duncan, K. Song, S. T. Hung, I. Miloradovic, A. Nayak, A. Persoons, T. Verbiest, M. J. Therien and K. Clays, *Angew. Chem., Int. Ed.*, 2008, **47**, 2978.
4. J. L. Bredas, C. Adant, P. Tackx, A. Petersoons and B. M. Pierce, *Chem. Rev.*, 1994, **94**, 243.
5. H. S. Nalwa, *Adv. Mater.*, 1993, **5**, 341.
6. M. Calvete, G. Y. Yang and M. Hanack, *Synt. Met.*, 2004, **141**, 231.
7. Z. B. Liu, Z. Guo, X. L. Zhang, J. Y. Zheng and J. G. Tian, *Carbon*, 2013, **51**, 419.
8. Z. B. Liu, J. G. Tian, Z. Guo, D. M. Ren, F. Du, J. Y. Zheng and Y. S. Chen, *Adv. Mater.*, 2008, **20**, 511.
9. A. J. Wang, L. L. Long, W. Zhao, Y. L. Song, M. G. Humphrey, M. P. Cifuentes, X. Z. Wu, Y. S. Fu, D. D. Zhang, X. F. Li and C. Zhang, *Carbon*, 2013, **53**, 327.
10. X. J. Liu, J. K. Feng, A. M. Ren and X. Zhou, *J. Mol. Struct.*, 2003, **635**, 191.
11. R. Misra, R. Kumar, V. PrabhuRaja and T. K. Chandrashekar, *J. Photochem. Photobiol. A*, 2005, **175**, 108; L. Jiang, Q. Chang, Q. Y. Ouyang, H. B. Liu, Y. X. Wang, X. R. Zhang, Y. L. Song and Y. L Li, *Chem. Phys.*, 2006, **324**, 556.
12. L. Jiang, F. S. Lu, H. M. Li, Q. Chang, Y. L. Li, H. B Liu, S. Wang, Y. L Song, G. L. Cui, N. Wang, X. R. He, D. B. Zhu, *J. Phys. Chem. B*, 2005, **109**, 6311.
13. L. Cronin and A. Müller, A themed issue on polyoxometalate chemistry in *Chem. Soc. Rev.,* 2012, **41,** pp9799-10106; D. Long and L. Cronin, A themed issue entitled Polyoxometalate Cluster Science in *Chem. Soc. Rev.,* 2012, **41,** pp 7325-7633.
14. A. Müller, E. Krickemeyer, H. Bögge, M. Schmidtmann and F. Peters, *Angew. Chem. Int. Ed.*, 1998, **37**, 3360.
15. L. J. Zhang, Y. S. Zhou and R. X. Han, *Eur. J. Inorg. Chem.*, 2010, **17**, 2471.
16. L. J. Zhang, Z. H. Shi, L. H. Zhang, Y. S. Zhou and S. Hassan, *Mater. Lett.*, 2012, **62**, 86.
17. Y. S. Zhou, Z. H. Shi, L. J. Zhang, S. Hassan and N. N. Qu, *Appl. Phys. A*, 2013, **113**, 563.
18. Y. S. Zhou, N. N. Qu, X. Wang, L. J. Zhang, Z. Shi and S. Hassan, *Chem. Res. Chin. Univ.*, 2014, **30**, 715.
19. C. Zou, Z. J. Zhang, X. Xu, Q. H. Guo, J. Li and C. D. Wu, *J. Am. Chem. Soc.*, 2012, **134**, 87.
20. Z. Liang, K. L. Dzienis, J. Xu, Q. Wang, *Adv. Funct. Mater.*, 2006, **16**, 542.
21. E. W. L. Chan, D. C. Lee, M. K. Ng, G. H. Wu, K. Y. C. Lee and L. P. Yu, *J. Am. Chem. Soc.*, 2002, **124**, 12238.
22. Z. H. Shi, Y. S. Zhou, L. J. Zhang, S. Hassan and N. N. Qu, *J. Phys. Chem. C*, 2014, **118**, 6413.
23. Z. H. Shi, Y. S. Zhou, L. J. Zhang, C. C. Mu, H. Z. Ren, S. Hassan, D. Yang and H. M. Asif, *RSC Adv.*, 2014, **4**, 50277.
24. M. Meot-Ner, A. D. Adler, *J. Am. Chem. Soc.*, 1975, **97**, 5107.
25. H. So, M. T. Pope, *Inorg. Chem.*, 1972, **11**, 1441.
26. Y. B. Yang, L. Xu, F. Y. Li, X. G. Du and Z. X. Sun, *J. Mater. Chem.*, 2010, **20**, 10835.
27. Y. B. Yang, L. Xu, B. B. Xu, X. G. Du and W. H. Guo, *Mater. Lett.*, 2009, **63**, 608.
28. C. D. Wagner, W. M. Riggs, L. E. Davis, J. F. Moulder and G. E. Muilenberg, Perkin-Elmer, Minnesota, 1979, Ch. 2, pp. 104-105.
29. K. Raymond, XPS peak fitting program for Windows, version 4.1, The Chinese University of Hong Kong, Hong Kong, China, 2000.
30. H. Yamashige, S. J. Matsuo, T. Kurisaki, R. C. C. Perera, H. Wakita, *Anal. Sci.*, 2005, **21**, 635.
31. A. Rani, K. A. Oh, H. Koo, H. J. Lee and M. Park, *Appl. Surf. Sci.*, 2011, **257**, 4982.

32. X. C. Ai, R. Jin, C. B. Ge, J. J. Wang, Y. H. Zou, X. W. Zhou and X. R. Xiao, *J. Chem. Phys*., 1997, **106**, 3387.
33. L. Xu, E. B. Wang, Z. Li, D. G. Kurth, X. G. Du, H. Y. Zhang and C. Qin, *New J. Chem*., 2002, **26**, 782.
34. M. Sheik-Bahae, A. Said, T. Wei, D. Hagan and E. V. Stryland, *IEEE. J. Quant. Electron*., 1990, **26**, 760.
35. Q. Y. Ouyang, H. L. Yu, H. Y. Wu, Z. Y. Lei, L. H. Qi and Y. J. Chen, *Opt. Mater*., 2013, **35**, 2352.
36. C. Yao, L. K. Yan, W. Guan, C. Liu, P. Song and Z. M. Su, *Dalton Trans*., 2010, 39, 7645.
37. R. L. Sutherland, Handbook of nonlinear optics, ed. B. J. Thompson, Marcel Dekker, Inc, New York, 2nd edn, 2003, ch. 6, pp. 356-360.

Porphyrin-polyoxometalate composite films fabricated using the versatile yet simple layer-by-layer approach show notable nonlinear saturated absorption and self-defocusing effects.